


# Modeling the Effect of Disruptions on the Absorber Treatment on Antenna Measurements

Vince Rodriguez<sup>1</sup>  FELLOW, AMTA  
(1) NSI-MI-TECHNOLOGIES, SUWANEE, GEORGIA, U.S.A

**Abstract**— Anechoic ranges require constant temperature and humidity, proper lighting to be able to work inside the range and closed-circuit television (CCTV) cameras to monitor the system while the measurement is being done. In addition, anechoic chambers require fire detection and suppression. Traditionally these penetrations are minimized and placed in non-critical areas. But the true effect of them has not been fully investigated. In this paper, antenna measurements as simulated in an indoor far field range. The approach to model the measurement is like the one the author presented in [1] and [2]. Thus, a range antenna (or near-field probe) and an antenna under test (AUT) are placed in free space and the AUT is rotated at discrete angles as it was done in [1]. Then a second model includes CCTV cameras, HVAC vents, light fixtures and both air sampling tubes and fire suppression nozzles and placed around. The simulation with these disruptions is repeated at the given discrete angles. The model does not include the absorber on the range. The model assumes a perfect absorber and the results of the simulated antenna measurement are compared to an ideal case with no disruptions. The results, while being approximations, provide a worst-case error for those disruptions of the RF-absorber layout. The results can be used to estimate the potential uncertainty on the measurement caused by the different systems that must be part of the anechoic enclosure. The technique is applied here to indoor far field measurements, and for near-field systems. Results show that for your typical roll over azimuth positioner, the effects of the penetrations on the ceiling are very small with differences in the -35 to -40 dB levels..

**Index Terms**— anechoic ranges, antenna measurements, computational electromagnetics, uncertainty

## I. INTRODUCTION

Anechoic ranges are the preferred environment to make antenna measurements. In these spaces, the interior surfaces are covered with radio-frequency (RF) absorber to simulate a free space environment. Ideally these RF absorber treatments would not have any disruptions. In reality, the anechoic ranges must have access doors, lights, CCTV cameras, fire detection sensors, and fire suppression systems among others. Ideally these are placed in areas, deemed by the engineer designing the absorber treatment, to be non-critical. The question remains, is there a way to model their effect, to obtain a level of the potential effect of these disruptions to at least provide a number to be used on the uncertainty analysis of the range?

While doing a complete analysis of the range may be impossible. It is possible to do a simplistic simulation to get an estimate of the effect of these structures on the antenna measurements. The simulation will allow to ignore other sources of error on the measurement and just study the effect of these structures.

## II. NUMERICAL APPROACH

A commercial method of moments (MoM) computational Electromagnetics (CEM) package is used to model the measurement of an antenna. This same package was used in [1]. As was the case in [1] and also in [3] the actual anechoic enclosure is not modeled. The assumption is that the absorber is perfect. Since the MoM does not require any absorbing or radiation boundaries, it is easy to set the model where only the range antenna and the AUT are present with the disturbances (see figure 1) By following this approach, reference [1] showed the effect of the AUT positioner absorber on the antenna being measured, while in reference [3] the effects of the feed fence on a compact antenna test range (CATR) quiet zone (QZ) metrics were computed. In the present paper, the effect of the disturbances on the measurement are calculated by comparing the cases with and without said disturbances.

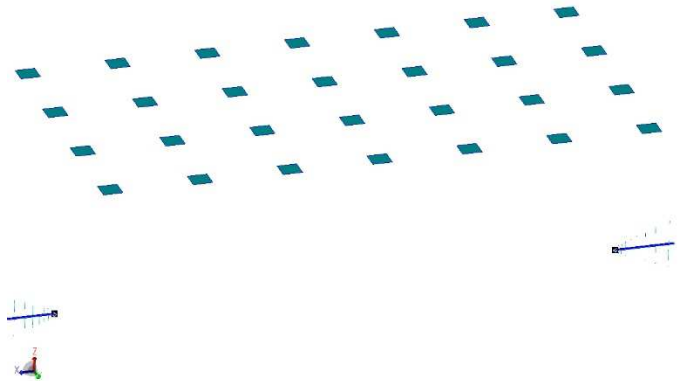


Figure 1: Two LPDA antennas inside a range with lights or vents at regular intervals on the ceiling.

## III. FAR FIELD RANGE

The first case assumes a range that is 39 ft (11.88 m) tall, by 46 ft wide (14 m) by 80 ft (24.38 m) long. The two identical Log Periodic Dipole Arrays (LPDA) are located 57.5 ft (17.5 m). The antennas are placed centerline in the range, thus they are 19.5 ft from the ground and 23 ft from the lateral walls. The center of rotation of the AUT is at the tip of the LPDA and it is located 11.25 ft (3.43 m) from the closest end wall. For the case with lights or vents on the ceiling, the vent/light is modeled with a 24 inch by 24 in (61 x 61 cm) perfect electric conductor (PEC) square. The “lights” are set on a 7 by 4 grid with a separation of

9.2 ft (2.8m) centered on the ceiling of the range. The AUT is rotated in Azimuth from 0° to 360° in 5° steps. The simulation is done for the antennas vertically and horizontally polarized. At each step the S21 is computed at 300, 400, and 500 MHz. Figure 2 shows the E and H patterns computed.

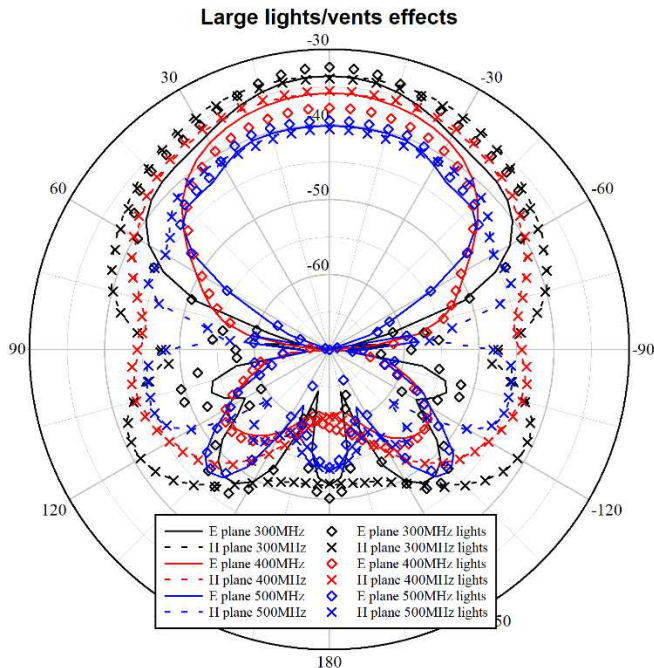


Figure 2: S<sub>21</sub> patterns for the LPDA at different frequencies for the case with no disturbances and the case with the disturbance present.

The data on Figure 2 show that there is significant change in the S<sub>21</sub> magnitude when the lights are present. Not only between the disturbance present and the perfect case, but also between the two polarizations of the case with the disturbance present. Since these antennas are identical, the following equation can be used to compute the gain

$$G = \frac{4\pi R \sqrt{|S_{21}|}}{\lambda} \quad (1)$$

Equation (1) is derived from the equations in [4]. Where G is the linear gain of each of the identical antennas and R is the distance between them. The computed gains are listed in TABLE I.

Table I: Computed Gains

Frequency (MHz)	Gain Free Space (dBi)	Gain E-plane (dBi)	Gain H plane (dBi)
300	6.68	7.26	6.50
400	6.78	5.81	6.93
500	5.57	5.92	5.35

The results show variations as large 0.91 dB (at 400MHz) between cases with the disturbances in place and the ideal case. The difference between the horizontal polarized case (E plane pattern) and the vertical polarized case (H plane patterns) is as large as 1.13dB (at 400MHz).

The difference on the measured patterns between the ideal case and the case with disruption is shown on figure 3

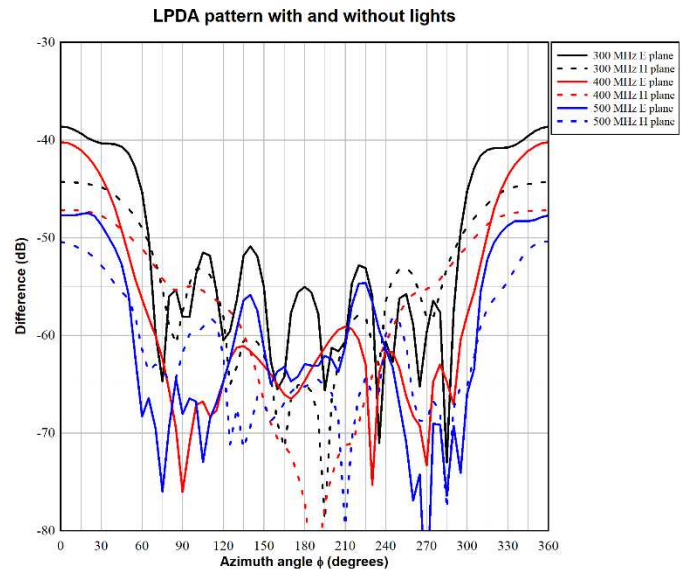


Figure 3: Difference expressed in dB between the cases with disturbances present and the free-space case.

While the data of figure 3 shows differences in the -38 dB to the -50 dB for the S<sub>21</sub> on the φ=0° direction, which is a small difference. However, the computation of the gain shows that this can lead to large errors on the measured gain. Figure 3, also shows that these differences are not constant around the pattern. The analysis done is a very simplistic and does not take into account the “shadowing” of these disturbances by the adjacent absorber, but it provides an approach to analyze the potential effect of these disturbances on measurement of gain. And helps in estimating the potential uncertainty due to these disturbances. A similar analysis could be performed with different antennas to simulate a three-antenna method [4] for measuring the gain or using a reference antenna to simulate the gain transfer method [4].

#### IV. NEAR FIELD RANGE

The second case analyzed is a standard spherical near field (SNF) range typically used for a minimum radiating sphere (MRS) with a maximum diameter of 70 cm. The measurement system is a roll over azimuth system. The probe used is an open-ended waveguide (OEWG) WR-284, and the simulations are conducted at 3 GHz. The system is placed in a rectangular range 14.33 ft (4.3 m) wide by 11.4 ft tall (3.47 m) tall, and 20.3 ft (6.18 m) long. The range centerline is 66.9 in (1.7 m) over the floor. The OEWG aperture is 70.2 in (1.78 m) from the center of rotation of the AUT. The center of rotation of the AUT is placed 91.45 in (2.3 m) from the back end-wall. The opposite end wall (behind the OEWG and probe stand) being 152 in (3.86 m) from the center of rotation. Figure 4 shows the model for this range with the AUT positioner, the probe positioner and the probe with the absorber collar. The fourth corner light is barely visible behind one of the ceiling HVAC vents. It should be noted, that



OEWG probe. The absorber is the same 5-inch pyramidal described in [5] with  $\epsilon_r=1.61+j1.41$ . The AUT is a small pyramidal horn with a WR-284 waveguide feed. The waveguide section is 2 inches long (5.08 cm) and the flare is 6 inches (15.24 cm) deep and the aperture is 7 inches by 5.75 inches (17.78 cm by 14.6 cm). The horn is positioned so that the azimuth rotation is performed around the plane between the waveguide and the flare.

### B. Simulations and results

As it was done on the previous case, the AUT is rotated every  $5^\circ$  from  $0^\circ$  to  $360^\circ$ . The rotation is performed for the vertical polarized case and for the horizontally polarized case. The results are compared to an ideal case with only the AUT and the probe and with a case with the positioners and no penetrations.

Figure 7 shows the data for the magnitude of the  $S_{21}$  for all the cases. There is not much appreciable difference between them except for the back lobe as expected and shown in [6]. This difference is the blockage from the positioner.

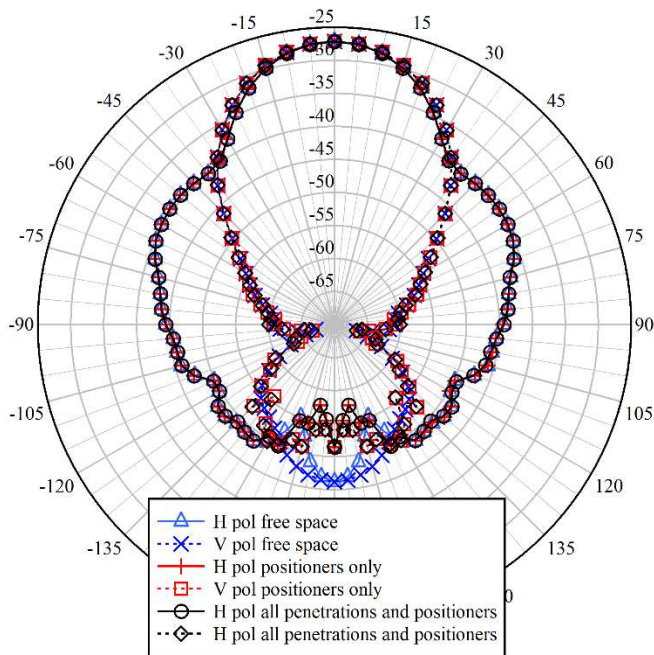


Figure 7: Magnitude of the  $S_{21}$  in dB plotted versus angle of rotation for both polarizations.

The phase of the  $S_{21}$  is shown in Figure 8. There are very slight differences on the phase. There are some orientations such as  $\phi=80^\circ$ ,  $115^\circ$ ,  $245^\circ$ ,  $280^\circ$ , where there is a significant difference in phase for the case with positioners and penetrations and the case with the positioner and no penetrations. These appear in the vertical polarization case, where the sidelobe seen in Figure 7, illuminates the ceiling.

A more thorough analysis is presented in Figure 9 where the difference in the linear magnitude of the  $S_{21}$  is presented in decibels. As reported in [6], the biggest difference comes from the blockage of the AUT positioner for the back lobe. However, in the main lobe direction differences can be seen in the -50 to -

60 dB range, not only between the cases versus the free space case, but also between the two cases where the only difference is the presence of the penetrations. There is some numerical uncertainty as well, so differences less than -60dB are effectively negligible. In general, the effect on the magnitude is very small ( $0.00001$  to  $0.000001$ ) and there are probably larger sources of error and uncertainty. Indeed the absorber reflectivity effects will be larger. It should be remembered that the design being analyzed places the penetrations in ideal locations.

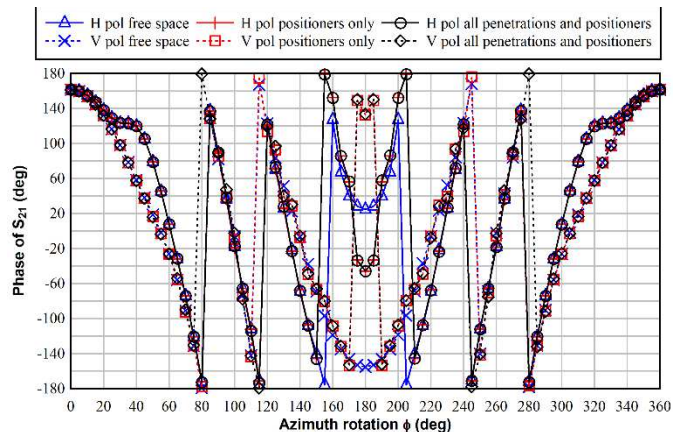


Figure 8: Phase of  $S_{21}$  plotted versus angle of rotation for both polarizations.

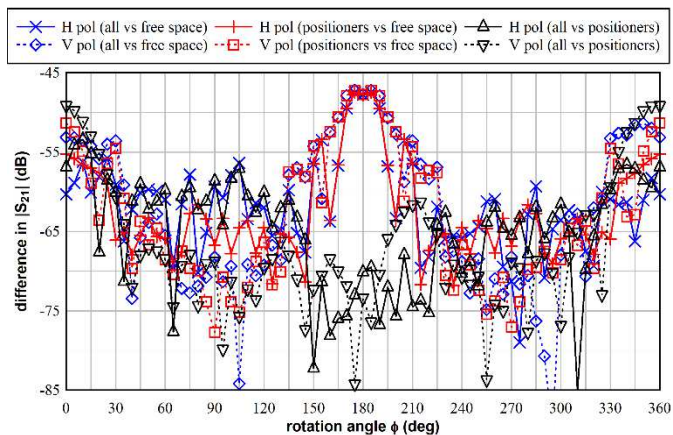


Figure 9: Difference of the magnitude of  $S_{21}$  in linear units expressed in dB and plotted versus the rotation angle for both polarizations.

Analyzing the differences in phase is important, as phase is critical for near to far field transformations. Figure 10. Show the phase difference of the range with penetrations and positioners compared to the free space case, and between the all penetrations and positioners to the case with the positioners only. The first case is plotted against the left y axis, while the second case is plotted against the right y axis.

On the first case the biggest difference is on the back lobe, where the blockage of the positioners causes a big difference

between the ideal free space case and the case where the AUT is supported by a positioner. A larger difference can be seen also for the H plane scan (vertical polarization) which is when the side lobes illuminate the ceiling where there are some of the disruptions such as the fire suppression and detection and also the lights and some of the HVAC vents.

On the second case, the difference is the presence of all the penetrations. The effect of these disruptions is small but in some orientations the difference is as large as  $8.6^\circ$ . The asymmetry of the penetrations is clearly observe on the phase difference.

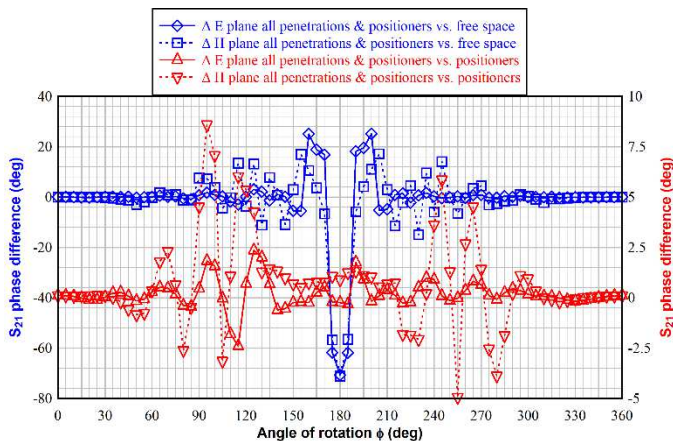


Figure 10: Difference of the phase of  $S_{21}$ . The case of all positioners and disruptions compared to the free space case is plotted against the left y axis. The case of the positioners and disruptions versus the case with positioners only is plotted on the right y axis. Data is plotted for all the rotation angles and for both polarizations.

## V. CONCLUSIONS

The authors have presented an approach to estimate the effect of penetrations and other disruptions of the absorber treatment in an anechoic range. Two cases are presented. The first case is a far field range with a large amount of lights or vents placed on the ceiling without regard for avoiding the specular region of the ceiling. The second case is a smaller SNF range where the penetrations are located avoiding the specular regions on the lateral surfaces of the range. The arrangement of the penetrations follows the best practice in anechoic range design. The effects shown are overestimated as there is no shadowing from the adjacent absorber as will be the case in the real range, however, the error or effect of these penetrations is calculated, for magnitude and phase. The results are not an exact solution. However, the numbers can be used for estimating uncertainties and for try to position the penetrations such that their effects are minimized.

## REFERENCES

[1] M. Ingerson, G. Dun and V. Rodriguez, "Effects of Antenna Under Test Positioner on the Measured Pattern of Antennas," 2024 IEEE International Symposium on Antennas and Propagation and INC/USNC - URSI Radio Science Meeting (AP-S/INC-USNC-URSI), Firenze, Italy, 2024, pp. 1835-1836.

[2] V. Rodriguez, A. Tellakula, D. J. van Rensburg and B. Mrdakovic, "Using a Higher-Order Basis Function based Method of Moments Analysis for

Designing Compact Antenna Test Ranges," 2022 Antenna Measurement Techniques Association Symposium (AMTA), Denver, CO, USA, 2022,

[3] V. Rodriguez, B. Mrdakovic, A. Tellakula, D. J. van Rensburg and M. Ingerson, "Analysis of the Feed Absorber Fences in Compact Antenna Test Ranges and their Impact on Quiet Zone Metrics," 2023 17th European Conference on Antennas and Propagation (EuCAP), Florence, Italy, 2023

[4] IEEE Recommended Practice for Antenna Measurements, IEEE Standard 149-2021, 2021

[5] V. Rodriguez, M. Ingerson and G. Dun, "On the RF Absorber Coverage of Antenna under Test Positioners," 2024 18th European Conference on Antennas and Propagation (EuCAP), Glasgow, United Kingdom, 2024, pp. 1-5, doi: 10.23919/EuCAP60739.2024.10501680.

[6] M. Ingerson, G. Dun and V. Rodriguez, "Effects of Antenna Under Test Positioner on the Measured Pattern of Antennas," 2024 IEEE International Symposium on Antennas and Propagation and INC/USNC - URSI Radio Science Meeting (AP-S/INC-USNC-URSI), Firenze, Italy, 2024, pp. 1835-1836, doi: 10.1109/AP-S/INC-USNC-URSI52054.2024.10686623.